Incorporation of texture in
multispectral synthetic image generation tools

J.R. Schott, C.N. Salvaggio, S.D. Brown, and R.A. Rose

Digital Imaging and Remote Sensing Laboratory
Center for Imaging Science
Rochester Institute of Technology
Rochester, New York

ABSTRACT

The Digital Imaging and Remote Sensing Synthetic Image Generation (DIRSIG) model emphasizes quantitative prediction of the radiance reaching sensors with bandpass values between 0.28 and 20.0 µm. The model embodies a rigorous end-to-end spectral modeling of radiation propagation, absorption and scattering, target temperatures based on meteorological history, extensive directional target-background interactions and detector responsivities.[1]

This paper describes texture quantification, the spectral-spatial correlation of textures, texture collection and generation methods. Finally, we will describe how DIRSIG generates texture on a pixel by pixel basis and maintains the spectral correlation of targets between bands.

1.0 Background

Synthetic image generation (SIG) models can be used to accurately simulate the myriad of real world variables and related phenomenology for the purpose of image system design, image exploitation algorithm testing, analyst training, and a variety of other valuable applications. The inherent value in using a SIG model lies in the ability of the user to control individual image generation parameters including detector geometry, target spectral signatures, time of day, meteorological history, atmosphere conditions, etc. Given proposed system parameters (including location, orientation, detector spectral sensitivities, optical geometries, etc.) SIG models can be used in the design stages of a sensor system to determine if desired phenomenology can be reliably captured under common operating conditions. This potentially decreases the overall development time of a given system by avoiding the construction of a prototype system and the analysis of lengthy test collections. These models can also be used to generate image sets for extensive testing of automated and semi-automated image exploitation algorithms. Additionally, these models provide a vehicle to test specific algorithm features by adjusting isolated image acquisition variables. As a training tool, SIG models can demonstrate what combinations of geometrical, meteorological, and thermodynamic conditions cause specific phenomenon to become apparent. In general, complex SIG models grant the ability to isolate specific elements in the imaging forming chain, and provide both the novice student and the expert analyst a tool to understand and validate the underlying principles involved.

Multispectral classification algorithms segment classes according to reflectance signatures which are assumed to be unique for a given class. This assumption can prove to be inadequate when unique classes with similar spectral signatures are encountered. In these cases, spatial signatures, or *textures*, can be incorporated to provide an additional or (in some cases) the exclusive criteria for classification. Aside from the value in land cover classification, textures represent a basic component in the human recognition of real-world targets. Therefore, for the visualization of *realistic-looking* synthetic targets used in analyst training, the incorporation of both spectral and spatial characteristics is desired.

The presence of texture within a specific land cover class arises, in large part, from variations in the target reflectance. For example, asphalt is not a homogenous material with a single spectral reflectance, but rather a heterogeneous mixture of several materials from a family of spectral reflectance curves. This family of spectral reflectances is characterized by specific multispectral statistics (*i.e.* mean vectors and covariance matrices) for that land cover class. Therefore, it is important for synthetic imagery used in multispectral classification or spectral segmentation algorithms to reproduce the appropriate multispectral statistics for each specific land cover class. Finally, it is important to recognize that textures in real scenes are also affected by topographic effects including cosine effects due to sun-target angles and variations in insolation (shadowing).

The Digital Imaging and Remote Sensing Lab's SIG model DIRSIG is a multispectral model that computes radiometric contributions across the user specified spectral bands simultaneously.[2] In fact, inherent to DIRSIG's design is the means to maintain spectral correlation since a single spectral curve is used for each radiance pixel. Furthermore, the DIRSIG model already accounts for self-shadowing, sun-target illumination variations and angular variations in target reflectances. Hence, the only task for the DIRSIG implementation was to develop a mechanism that selects reflectance curves on a pixel-by-pixel basis, thereby preserving the spatial correlation of the template texture image and the spectral correlation across multispectral bands.

2.0 The Spatial/Spectral Correlation Approach

The proposed multispectral hybrid texture technique utilizes a texture image from a defined bandpass to drive the selection of a reflectance curve (from a large family of curves) to be used across all bandpasses for that pixel. The template texture image appropriate for the given land cover class can come from a variety of sources. For instance, a gaussian random texture would produce fairly "good looking" results for a gravel roof imaged at a spatial resolution on the order of several inches per pixel. This same approach, however, would not be adequate for more structured texture patterns such as row crops, parking areas, or mowed grass. These types of textures can be synthetically generated using fractal-based or other deterministic techniques which require substantial compute time and lack the index of control needed for our application. The most readily available source of texture is often actual imagery of the specific land cover class. For the examples presented in this paper, actual single band images of the desired target classes were used as the source of texture patterns for the scene generation process.

A mechanism had to be developed to link the grey value in a texture image to a given spectral curve in a large family of spectral curves. We used the statistical relationship between the variance of the pixels in the texture image and the variance of the reflectance curves in the texture image bandpass. This mechanism was implemented with an efficient run-time approach and minimal amount of data preparation before run-time. The pre-run calculations include ranking the entire family of reflectances curves for a given land cover class in the spectral band sampled by the texture image (c.f. Figure 1). This ranking is accomplished by computing the mean spectral reflectance of all the curves for that specific class as:

$$\rho_{avg,i} = \frac{\sum_{\lambda=\lambda_{min}}^{\lambda_{max}} \rho_{\lambda,i}}{n_i} \tag{1}$$

for $i = 1, N$ where $\rho_{avg,i}$ is the average reflectance over the bandpass from λ_{min} to λ_{max} for the ith curve in the family of N curves, $\rho_{\lambda,i}$ is the spectral reflectance for the ith curve at λ, and n_i is the number of points across the bandpass for the ith curve. The mean and standard deviation for the bandpass averages are then computed as:

$$\rho_{avg} = \frac{\sum_{i=1}^{N} \rho_{avg,i}}{N} \tag{2}$$

and

$$\sigma_\rho = \sqrt{\frac{\sum_{i=1}^{N} (\rho_{avg,i} - \rho_{avg})^2}{N-1}} \tag{3}$$

Once these statistics are determined, the curves are ranked by assigning each curve a z-score which is computed as:

$$z_i = \frac{\rho_{avg,i} - \rho_{avg}}{\sigma_\rho} \tag{4}$$

The z-scores are then used to select the proper curve to use for a particular brightness in the material specific texture image (c.f. Figure 1).
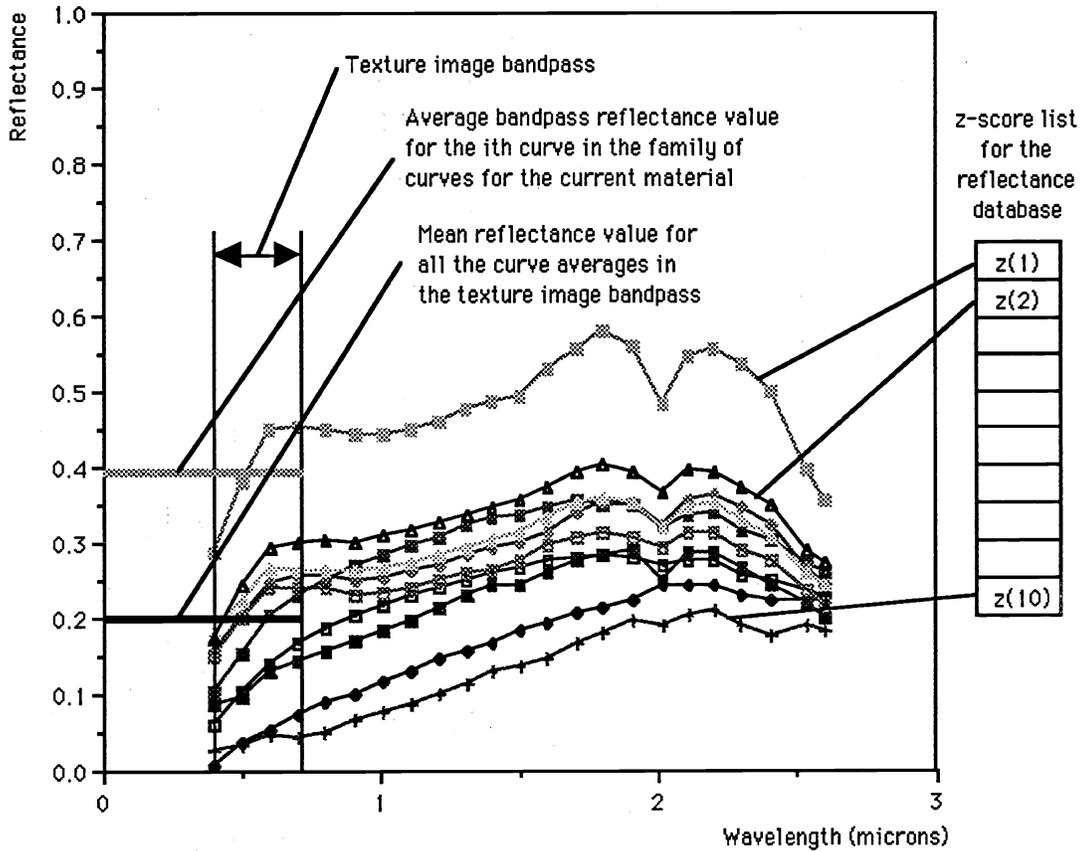

Figure 1: Ranking of reflectance curves by z-score in the bandpass defined by the texture image for that land cover.
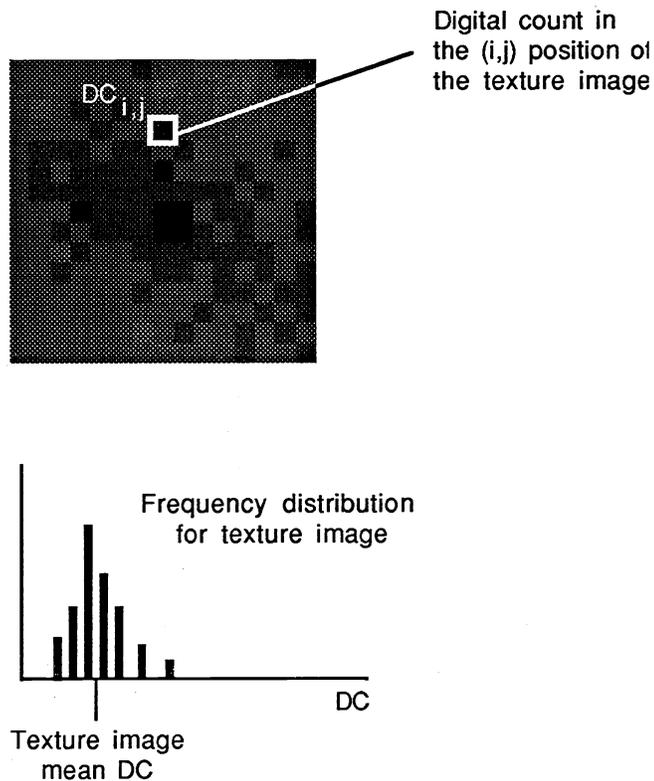
During the actual scene generation process, a pixel is retrieved from the texture image and the z-score ($z_{texture}$) is computed using the mean ($\mu_{texture}$) and standard deviation ($\sigma_{texture}$) of the entire texture image as (c.f. Figure 2):

$$z_{texture} = \frac{DC_{i,j} - \mu_{texture}}{\sigma_{texture}} \tag{5}$$

The reflectance curve for the synthetic pixel is then selected by matching the resulting texture image z-score to the z-scores of the reflectance curves in the database.

3.0 Generation of Large Reflectance Curve Sets

Commonly a large family of reflectance curves are not available for use with this type of multispectral texture treatment. Therefore, a technique was developed to produce an arbitrary number of spectral curves from a smaller set of curves containing the desired multivariate statistics for the given land cover class. This technique entails generating, for each land cover class, a mean vector containing an entry for each spectral point in the reflectance database and a covariance matrix containing the variance between each spectral point in the class. The spectral points are zero-centered by subtracting the mean vector and are then transformed into a spectrally non-correlated space. The creation of new curves involves generating normally distributed random samples in the non-correlated space using the eigen values of the variables in the transformed

Digital count in
the (i,j) position of
the texture image

Frequency distribution
for texture image

DC

Texture image
mean DC

Figure 2: The z-score from the pixel at position (i,j) in the texture image is determined using the grey-level distribution for this texture image.

space to define the standard deviation for each sample set. These sample sets (vectors) are then back transformed into the spectrally correlated space where they exhibit the same spectral characteristics as the base set.

This approach proceeds as follows. From a set of actual spectral curves representative of a land cover class (material type) which is assumed to be distributed as $N_{396}(\bar{\mu}, \bar{\Sigma})$ (*i.e.* a multivariate normal distribution with mean $\bar{\mu}$ and covariance $\bar{\Sigma}$), the mean vector and covariance matrix are calculated at the full DIRSIG spectral resolution (396 data points) given by:

$$\bar{\mu}^t = \begin{bmatrix} \mu_0 & \mu_1 & \mu_2 & \cdots & \mu_{395} \end{bmatrix},$$

(6)

and

$$\bar{\Sigma} = \begin{bmatrix} \sigma_{0,0} & \sigma_{0,1} & \sigma_{0,2} & \cdots & \sigma_{0,395} \\ \sigma_{1,0} & \sigma_{1,1} & \sigma_{1,2} & \cdots & \sigma_{1,395} \\ \sigma_{2,0} & \sigma_{2,1} & \sigma_{2,2} & \cdots & \sigma_{2,395} \\ \vdots & \vdots & \vdots & \ddots & \vdots \\ \sigma_{395,0} & \sigma_{395,1} & \sigma_{395,2} & \cdots & \sigma_{395,395} \end{bmatrix}$$

(7)

where $\bar{\mu}$ and $\bar{\Sigma}$ are the mean vector and covariance matrix for an individual class, μ_n is the mean for the nth point of the spectra, and $\sigma_{i,j}$ is the covariance between the ith and j^{th} spectral means for this class. One can compute the eigen values and eigen vectors for the covariance matrix, $\bar{\Sigma}$, to obtain the following:

$$\vec{\lambda}^t = \begin{bmatrix} \lambda_0 & \lambda_1 & \lambda_2 & \cdots & \lambda_{395} \end{bmatrix}, \tag{8a}$$

$$\vec{e} = \begin{bmatrix} e_{0,0} & e_{1,0} & e_{2,0} & \cdots & e_{395,0} \\ e_{0,1} & e_{1,1} & e_{2,1} & \cdots & e_{395,1} \\ e_{0,2} & e_{1,2} & e_{2,2} & \cdots & e_{395,2} \\ \vdots & \vdots & \vdots & \ddots & \vdots \\ e_{0.395} & e_{1,395} & e_{2,395} & \cdots & e_{395,395} \end{bmatrix} \tag{8b}$$

where $\lambda_0 \geq \lambda_1 \geq \lambda_2 \geq \cdots \geq \lambda_{395} \geq 0$ and the columns of $\vec{e}$ contain the normalized eigen vectors corresponding to the eigen values, $\vec{\lambda}$, for an individual land cover class.

We know that if the zero-centered original data was transformed via its eigen vector matrix, $\vec{e}$, as:

$$\vec{Y} = \vec{e}^{\,t}(\vec{X} - \bar{\mu}) \tag{9}$$

where $\vec{X}^t = \begin{bmatrix} x_0 & x_1 & x_2 & \cdots & x_{395} \end{bmatrix}$ are the original spectral curves, one would obtain a data set, $\vec{Y}$, which was spectrally non-correlated. This non-correlated data set would be distributed as $N_{396}(\vec{0}, \bar{\Lambda})$ where the covariance matrix, $\bar{\Lambda}$, has the form:

$$\bar{\Lambda} = \vec{e}^{\,t} \bar{\Sigma} \vec{e} = \begin{bmatrix} \lambda_0 & 0 & 0 & \cdots & 0 \\ 0 & \lambda_1 & 0 & \cdots & 0 \\ 0 & 0 & \lambda_2 & \cdots & 0 \\ \vdots & \vdots & \vdots & \ddots & \vdots \\ 0 & 0 & 0 & \cdots & \lambda_{395} \end{bmatrix} \tag{10}$$

This non-correlated covariance matrix is used to generate multivariate random variables distributed as $N_{396}(\bar{\mu}, \bar{\Sigma})$. To do this, we generate a set of gaussian-distributed random numbers, y_i, distributed as $N(0, \lambda_i)$ for ($i = 0,1,2, ..., 395$) to form the vector

$$\hat{\vec{Y}} = \begin{bmatrix} y_0 & y_1 & y_2 & \cdots & y_{395} \end{bmatrix} \tag{11}$$

This vector is then back transformed through the inverse of Equation 9 according to:

$$\hat{\vec{X}} = (\vec{e}^{\,t})^{-1} \hat{\vec{Y}} + \bar{\mu} \tag{12}$$

to yield a multivariate random variable distributed as $N_{396}(\bar{\mu}, \bar{\Sigma})$ which could be used to represent a reflectance curve from a population with these multivariate statistics.
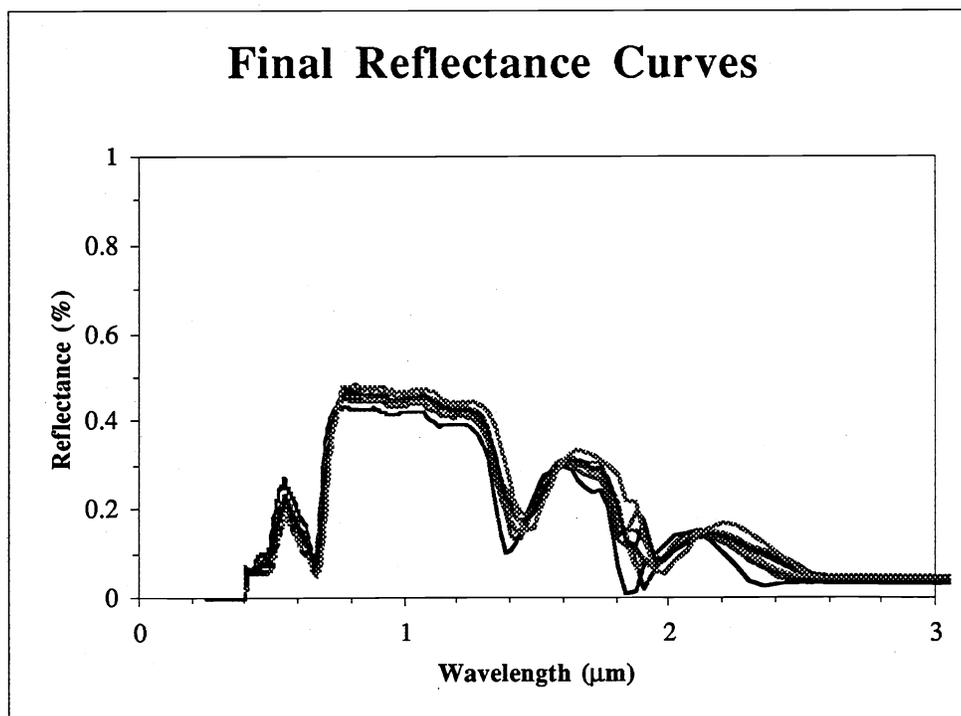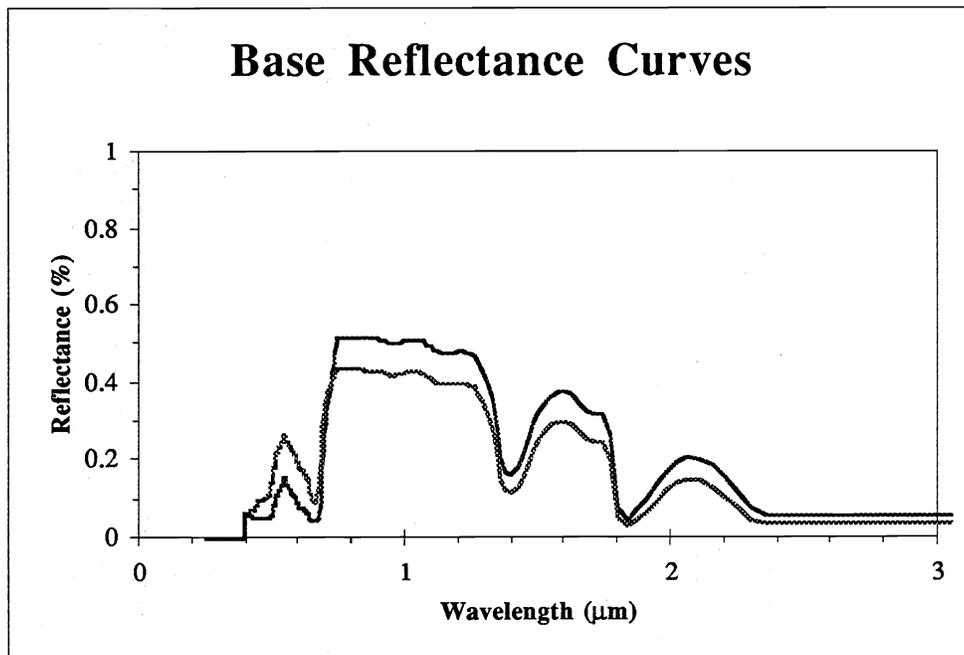
Figure 3: A subset of base curves (top) and a subset of final curves (bottom) generated using the described approach.

These procedures can be used to produce an arbitrarily large family of curves (*c.f.* Figure 3). The number of curves to be generated for a particular material is at the user's discretion. It should be noted, however, that in order to obtain a statistical match of the specified multivariate normal statistics with those exhibited by the generated curve set, a large number of curves will need to be generated (e.g. output populations sizes of 100 curves are not unusual).

4.0 Results and Recommendations

The development effort to date has been focused on the radiometric aspects of including texture in the DIRSIG model and preserving the spatial and spectral correlation of the material. The imagery resulting from the use of this technique has reproduced the desired texturing effects while maintaining the mean level integrity of the radiometry model. The approach as currently implemented introduces essentially no incremental run time. However, the user must supply template texture images which are at the appropriate scale and orientation for each land cover class being generated. Future enhancements should include the preparation of texture images to automatically account for these simple geometric and scale effects.
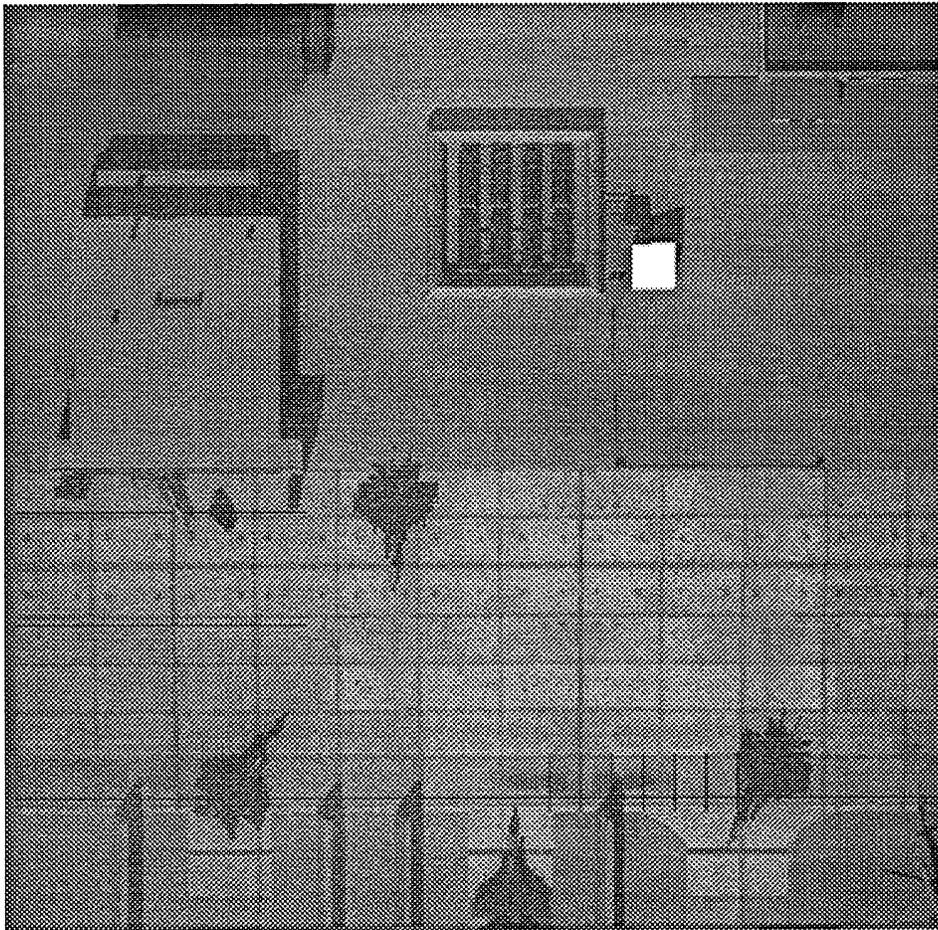
Figure 4: A DIRSIG pan visible (top) image of a scene featuring concrete, grass, and gravel roof textures.
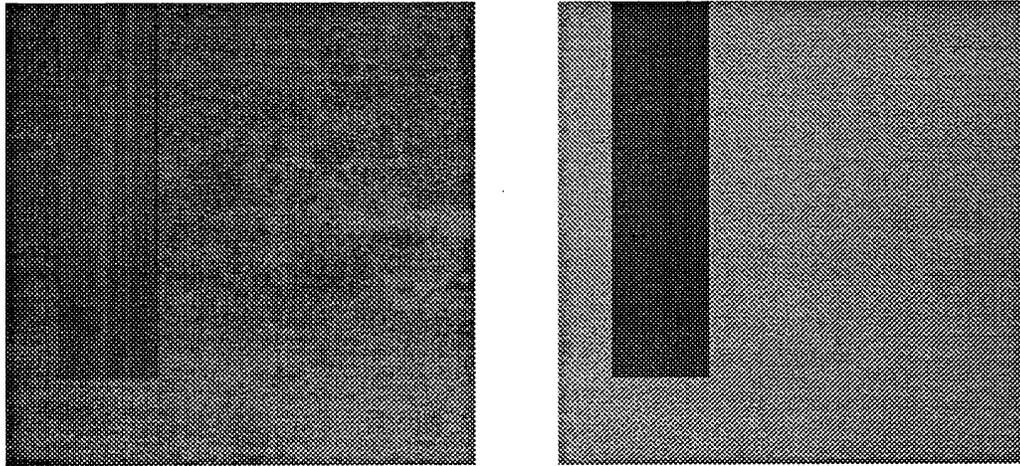
Figure 5:
Contrast enhanced DIRSIG images in the green (left) and near IR (right) bands of an image of an asphalt runway and grass. Note the positive correlation between the asphalt and the stained region in the lower-left. The stain is darker in both cases. In contrast, note the areas in the grass that are bright in the green band are dark in the near IR. This is characteristic of the spectral behavior of vegetation reproduced by the DIRSIG treatment presented here.

The evaluation of the images to this point has been completely subjective. Future efforts should be directed at evaluating the integrity of the texture images in a more quantitative fashion. These efforts should also focus on evaluation of the use of texture in a hybrid or layered fashion. This would be applicable to geometrically structured surfaces such as tree canopies. In this case the low frequency structure (*e.g.* major branch and crown structuring) might be built into the 3D geometry of the synthetic object. Higher frequency texture (*e.g.* minor branch and leaf structure) would be introduced by the methods presented here.

In summary an approach has been developed and demonstrated that simultaneously preserves the spectral and spatial correlation in multispectral synthetic imagery. This is critical to accurate modeling of synthetic scenes for use in algorithm development and evaluation.

5.0 References

1.   Schott, J.R., Raqueno, R., and Salvaggio, C., "Incorporation of a Time-Dependent Thermodynamic Model and Radiation Propagation Model into Infrared Three-Dimensional Synthetic Image Generation", *Optical Engineering*, Vol. 37, No 7., 1505, July 1992.

2.   Schott, J.R., and Salvaggio, C., "MODTRAN Version of DIRSIG Software:, SIDE Report 92-51-101, 1992.

3.   Schott, J.R., Mason, J.E., Salvaggio, C., Sirianni, J.D., Rose, R.A., Kulp, E.O., Rankin-Parobek, D., "DIRSIG - Digital Imaging and Remote Sensing Image Generation Model; Description Enhancements, and Validation", RIT/DIRS Report 92/93-51-146, July, 1993.

4.   Mason, J.E., Schott, J.R., and Rankin-Parobek, D., "Validation analysis of the thermal and radiometric integrity of RIT's synthetic image generation model, DIRSIG", Proceedings of SPIE Vol. 2223, page 474-487, Orlando, April 1994a.

5.   Mason, J.E., Schott, J.R., Salvaggio, C., and Sirianni, J.D., "Validation of the contrast and phenomenology in the Digital Imaging and Remote Sensing (DIRS) Lab's Image Generation (DIRSIG) model", Proceedings of the SPIE Annual Meeting on Optics, Imaging and Instrumentation, Vol. 2269, #72, San Diego, CA, 1994b.